SAND2016-1001C

Generation-After-Next Power Electronics Using Ultra-Wide-Bandgap Semiconductors

Robert J. Kaplar, Andrew A. Allerman, Andrew M. Armstrong, Arthur J. Fischer, Jeramy R. Dickerson, Michael P. King, Albert G. Baca, and Mary H. Crawford
Sandia National Laboratories
Albuquerque, NM 87185, USA

Abstract: *This paper describes the merits of the so-called "ultra-wide-bandgap" materials with bandgaps larger than that of GaN (3.4 eV) for power electronics applications, with a particular focus on the Aluminum Gallium Nitride (AlGaN) materials family. High-voltage vertical GaN and AlGaN PiN diodes are demonstrated to have breakdown voltages of approximately 3.9 and 1.5 kV, respectively. Furthermore, two-dimensional electron gases are shown to exist in AlGaN heterostructures with aluminum composition >70%, as required to achieve conductivity in the channel of a transistor. To our knowledge, this is the first report of such results in AlGaN.*

Keywords: Power electronics; ultra-wide-bandgap; Aluminum Gallium Nitride, PiN diode; heterostructure.

Introduction

Dramatic improvements in Size, Weight, and Power (SWaP) for power conversion systems have recently been enabled by the adoption of Silicon Carbide (SiC) and Gallium Nitride (GaN) based power switching devices [1-5]. Despite significant progress in Wide-Bandgap (WBG) materials and the dramatic advantages conferred by them relative to the incumbent Silicon (Si) based technology, various challenges related to performance and reliability remain. For example, SiC MOSFETs have suffered from low channel mobility [6,7] and gate oxide reliability problems [8], while non-MOS SiC devices such as JFETs may not be normally-off [2]; similarly, GaN-channel HEMTs are intrinsically normally-on, and normally-off operation requires complex gate stack processing that may degrade long-term device reliability [4]. Lateral GaN HEMTs are also limited in breakdown voltage [9], and do not exhibit avalanche behavior. Consequently, these devices must be over-designed to ensure reliable operation. Improvement in WBG material and device technology has slowed as the technology has matured and become commercially available, and fundamental material properties now limit performance. Thus, dramatic leaps in power electronics require a new generation of materials, the so-called "Ultra" Wide-Bandgap (UWBG) materials with bandgaps larger than 3.4 eV. This paper presents highlights of Sandia National Laboratories' efforts to develop the Aluminum Gallium Nitride (AlGaN) system into a viable material for generation-after-next power electronics.

A variety of "Figures of Merit" (FOM) are often used to compare materials for power semiconductor devices. The most common of these is the so-called "unipolar" FOM, defined by [10]:

$$\frac{V_B^2}{R_{on,sp}} = \frac{\varepsilon \mu_n E_C^3}{4} \quad [1]$$

where V_B is the avalanche breakdown voltage due to impact ionization [11] in the off-state, $R_{on,sp}$ is the resistance of the device in the on-state multiplied by the device area (i.e. the so-called "specific" on-resistance), ε is the material's permittivity, μ_n is the electron mobility, and E_C is the "critical electric field", which is defined as the maximum field in a one-sided junction at the onset of avalanche breakdown. In such a junction, the electric field profile is a linear function of position, and the maximum field occurs at the junction itself. This is the strict definition of E_C, but it is often misinterpreted as the field which, when exceeded anywhere in a device of arbitrary geometry, leads to breakdown (whether by avalanche or some other process); despite this lack of rigor, the concept of the critical field is nevertheless a convenient metric by which to compare the merits of different materials for power devices. Strictly speaking, Equation 1 is only valid for an infinite planar junction, but it is often used as a universal comparison for power devices of arbitrary geometry (indeed, a different FOM can be derived for lateral devices [3,12]); the approach taken in this paper is to utilize the standard unipolar FOM, in order to facilitate easy comparison to the majority of the WBG power electronics literature.

The most important aspect of Equation 1 is that the FOM scales as the cube of the critical field. The critical field, in turn, is a strong function of the bandgap. Hudgens *et al*. [13] have reported that the critical field scales as the square of the bandgap for indirect-gap semiconductors and as the 2.5 power of the bandgap for direct-gap semiconductors. These dependencies are plotted in Figure 1; the predicted critical fields of a few semiconductors of interest are also noted on the plot. These curves are calculated from the empirical relationships given in Reference 13, which are based on measurements of a variety of semiconductors. However, it is possible that the dependence of the critical field on bandgap is even stronger for AlGaN, due to the predicted lessening of the hole impact ionization coefficient relative to the electron impact ionization coefficient as the bandgap is increased [14]. In theory, a device constructed out of a material in

which only the electron impact ionization coefficient is non-zero will never avalanche [15]; of course, it will eventually fail by some other high-field related mechanism (e.g. dielectric breakdown of the surface passivation).

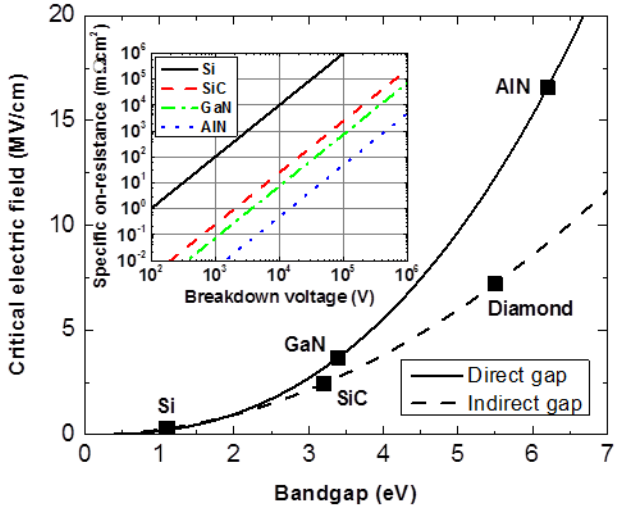

Figure 1. Main figure: Postulated dependence of the critical electric field on bandgap for direct-gap and indirect-gap semiconductors, after Hudgens et al. [13]. Inset: Unipolar figure-of-merit for Si, SiC, GaN, and AlN.

The predicted dependence of E_C on bandgap, combined with Equation 1, implies that the FOM scales between the 6 and the 7.5 power of the bandgap. To be conservative, assume that the scaling power is 6. All other things being equal, comparing conventional Si to the WBG material GaN, one predicts a factor of $(3.4/1.1)^6 \approx 870$ improvement in the FOM! Further comparing UWBG Aluminum Nitride (AlN) to GaN, an additional factor of $(6.2/3.4)^6 \approx 37$ improvement is anticipated. The predicted FOM curves ($R_{on,sp}$ vs. V_B) for Si, SiC, GaN, and AlN are plotted in the inset of Figure 1. Other factors in Equation 1 also depend on bandgap; for example, the electron mobility in AlGaN will be less than that in GaN due to alloying effects [12]. Additional issues such as the size, quality, and cost of native substrates [16] as well as the ability to selectively and controllably dope WBG and UWBG materials (e.g. ion implantation is difficult in GaN [17], and the Si dopant becomes very deep in Al-rich AlGaN [18]) are likewise challenges. Further, Si enjoys a tremendous advantage in terms of process maturity even compared to "conventional" WBG materials such as SiC, let alone an emerging material such as AlN. Nevertheless, the extremely strong dependence of the FOM on bandgap makes a compelling case for the investigation of UWBG materials for power electronics. This is especially true for very demanding applications such as pulsed power, where extremely high power is required in a constrained volume for a very short time, the market is small but critically important, and cost may not be a primary constraint.

GaN and AlGaN PiN Diodes

Due to the recent availability of conducting GaN substrates, vertical GaN power devices are now possible and have been reported by a number of groups [19-25]. As an initial set of work on vertical power devices, Sandia has fabricated and tested GaN PiN diodes grown on GaN substrates. The *I-V* characteristic of a representative high-voltage GaN diode is shown in Figure 2. The diode was grown by Metal-Organic Chemical Vapor Deposition (MOCVD) and has a drift region thickness of approximately 15 μm with net *n*-type doping in the mid-10^{15} cm^{-3} range. The diode processing included edge termination to mitigate early breakdown [25]. The main part of the figure shows the reverse *I-V* characteristic on a linear scale, where the breakdown at approximately 3.9 kV is evident. This breakdown is reversible and is suggestive of impact-ionization-induced avalanche breakdown, consistent with previous work on similar diodes [26]. The inset shows the forward *I-V* characteristic; a low specific on-resistance of $R_{on,sp} \approx 1.9$ $m\Omega \cdot cm^2$ was extracted from this curve.

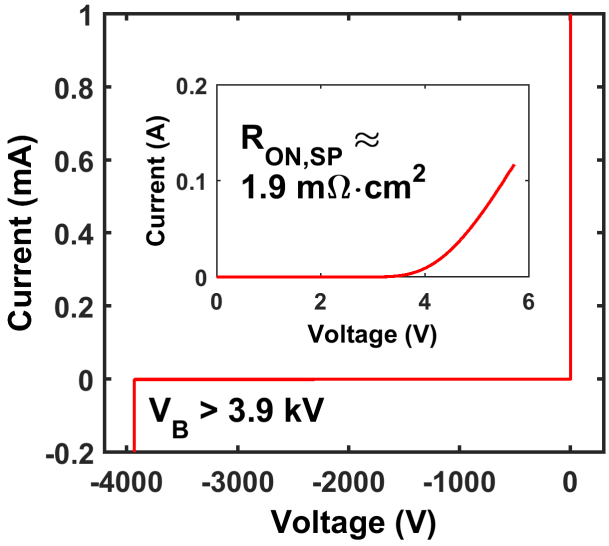

Figure 2. Main figure: IV characteristic of vertical GaN PiN diode grown by MOCVD on GaN substrate. Inset: Forward IV characteristic of same diode.

Figure 3 shows (V_B, $R_{on,sp}$) pairs measured for several Sandia GaN PiN diodes, as well as values reported in the literature from a number of groups. Further, the calculated GaN unipolar FOM is shown for several assumed values of the critical electric field; for these calculations μ_n = 1200 $cm^2/V \cdot s$, which is quite conservative compared to recently reported results [21]. Comparison of the data to the calculated curves indicates that the critical electric field for GaN may be as high as 4 MV/cm.

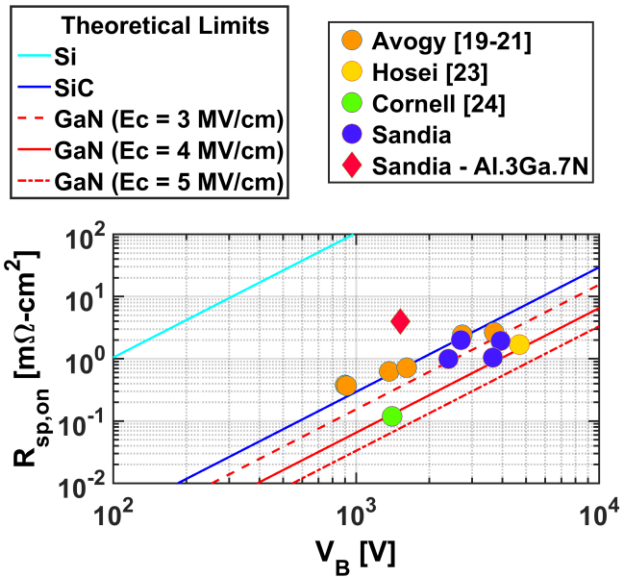

Figure 3. Measured (V_B, $R_{on,sp}$) pairs for Sandia-fabricated GaN PiN diodes, compared to literature values as well as theoretical $R_{on,sp}$ *vs.* V_B FOM curves calculated assuming various values of the critical electric field for GaN. Sandia $Al_{0.3}Ga_{0.7}N$ PiN diode is also shown.

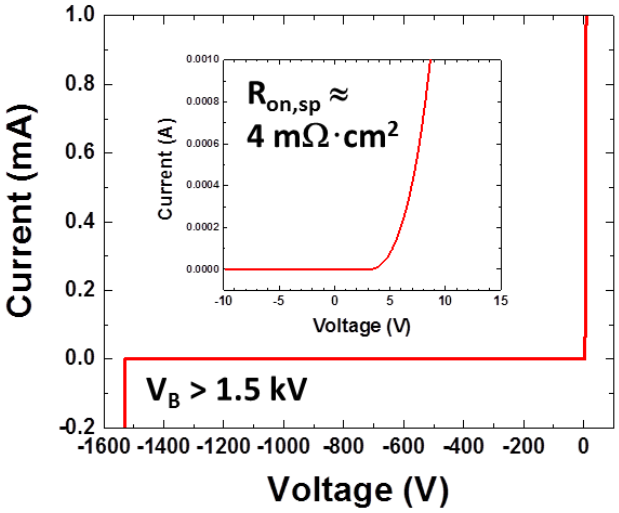

Figure 4. Main figure: IV characteristic of quasi-vertical $Al_{0.3}Ga_{0.7}N$ PiN diode grown by MOCVD on AlN template on sapphire. Inset: Forward IV characteristic of same diode.

With the true goal being the demonstration of UWBG devices, $Al_{0.3}Ga_{0.7}N$ PiN diodes were also grown and processed. An aluminum mole fraction of 0.30 was used for this initial UWBG diode due to the relative ease of doping 30% material compared to more Al-rich material [18]. The AlGaN diodes were grown by MOCVD on AlN templates on thick sapphire substrates, developed for previous UV optoelectronics work [27]. Due to the insulating nature of the sapphire substrate, these vertical diodes are mesa-etched and the *n*-contact is deposited to the side of the mesa on the top surface of the wafer such that the diode assumes a "quasi-vertical" configuration. An *I-V* characteristic of a representative $Al_{0.3}Ga_{0.7}N$ diode is shown in Figure 4. The drift region thickness for the diode shown is ~ 4 μm, with net *n*-type doping in the low 10^{16} cm^{-3} range. V_B > 15 kV and $R_{on,sp}$ ~ 4 mΩ·cm^2 is achieved. To our knowledge, this is the first report of a high-voltage vertical AlGaN PiN diode.

Al-Rich AlGaN Heterostructures

In contrast to the vertical devices described above, lateral devices may be achieved using thinner Al-rich epilayers and do not require *pn* junctions. Thus, a three-terminal power transistor based on Al-rich AlGaN is most likely to be achieved first in a lateral device configuration, e.g. using a Heterostructure Field-Effect Transistor (HFET) architecture wherein a 2-Dimensional Electron Gas (2DEG) conducting channel formed at the interface between layers of differing bandgap is utilized to carry the current. Thus, the goal is to use an $Al_xGa_{1-x}N$ channel layer in conjunction with a wider-bandgap $Al_yGa_{1-y}N$ barrier ($y > x$). A number of groups have previously reported on both experimental [28-35] and computational [12,36] work on similar structures. Among the experimental papers, the highest Al% reported was an $AlN/Al_{0.60}Ga_{0.40}N$ barrier/channel structure [35]; in contrast, our focus is on heterostructures with channel Al composition > 70%.

We have grown by MOCVD a number of Al-rich heterostructures such as described above, intended for processing into power switching devices. These heterostructures were grown on patterned AlGaN templates on thick sapphire [27]. Barrier/channel heterostructures of two compositions were grown: $Al_{0.85}Ga_{0.15}N/Al_{0.70}Ga_{0.30}N$ and $AlN/Al_{0.85}Ga_{0.15}N$. As a representative example, a capacitance-voltage (*C-V*) curve was obtained using a mercury probe on an $AlN/Al_{0.85}Ga_{0.15}N$ heterostructure with a 40 nm thick Si-doped barrier, and the carrier density vs. depth was extracted from this curve, as shown in Figure 5. The exponential drop in charge density between 30 and 70 nm provides evidence that a 2DEG is present in the heterostructure (this is also apparent in a similar plot for the $Al_{0.85}Ga_{0.15}N/Al_{0.70}Ga_{0.30}N$ Si-doped heterostructure), and to our knowledge this is the first demonstration of a 2DEG channel layer in an $Al_yGa_{1-y}N/Al_xGa_{1-x}N$ heterostructure with $y > x > 0.7$.

Contactless sheet resistance measurements were made on the heterostructure, and coupled with the *C-V* measurements the following values were obtained: Sheet resistance R_{sh} ≈ 10 kΩ/square, 2DEG density n_s ≈ 2.4×10^{12} cm^{-2}, and channel mobility μ_n ≈ 250 $cm^2/V\cdot s$. Assuming source-to-gate length L_{SG} = 1.0 μm, gate length L_G = 1.0 μm, and gate-to-drain length L_{GD} = 12.5 μm (consistent with dimensions commonly utilized in

conventional GaN-channel power switching devices [9]), these values are not far from those necessary to achieve a 5 kV, 5 mΩ·cm^2 switch; such a device would match the theoretical performance of SiC. Si-doped heterostructures of varying barrier thickness were also grown, and the pinch-off voltage was observed to move closer to zero for thinner barriers, as is the case for conventional GaN-channel heterostructures [37]. This provides the possibility, when combined with a high Schottky barrier height, to achieve an intrinsically normally-off device. 2DEGs were also observed in heterostructures of both compositions but without intentional Si doping in the barrier.

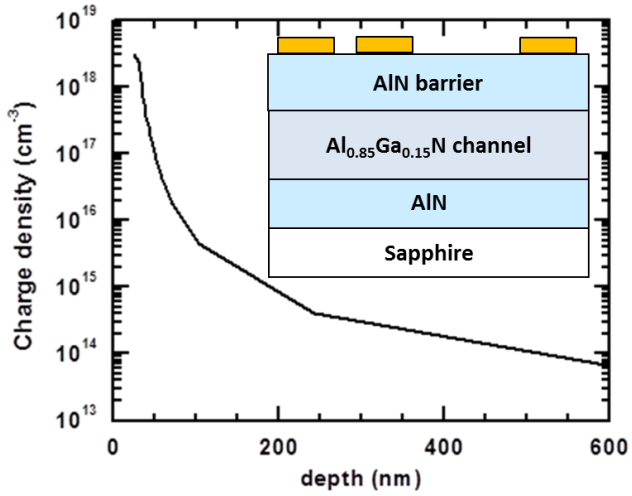

Figure 5. Main figure: Carrier density vs. depth for AlN/$Al_{0.85}Ga_{0.15}N$ barrier/channel heterostructure with a 40 nm thick Si-doped barrier. Inset: Schematic of structure.

Acknowledgements

The authors thank J. Wierer of Lehigh University for collaboration on the GaN PiN diode work, J. Neely of Sandia for discussions concerning applications of the devices described herein and for reviewing the manuscript, and I. Kizilyalli of Avogy for numerous fruitful discussions concerning GaN PiN diodes. This work was supported by the Laboratory Directed Research and Development (LDRD) program at Sandia. Sandia National Laboratories is a multi-program laboratory managed and operated by Sandia Corporation, a wholly owned subsidiary of Lockheed Martin Corporation, for the U.S. Department of Energy's National Nuclear Security Administration under contract DE-AC04-94AL85000.

References

1. D. K. Schroder, *Int. J. High Speed Elec. Sys.* **21**(1), 1250009 (2012).
2. V. Veliadis et al., *IEEE Elec. Dev. Lett.* **34**(3), 384 (2013).
3. B. J. Baliga, *Semi. Sci. Tech.* **28**, 074011 (2013).
4. M. Su et al., *Semi. Sci. Tech.* **28**, 074012 (2013).
5. M. J. Scott et al., *Semi. Sci. Tech.* **28**, 0774013 (2013).
6. Y. K. Sharma et al., *IEEE Elec. Dev. Lett.* **34**(2), 175 (2013).
7. G. Liu et al., *IEEE Elec. Dev. Lett.* **34**(2), 181 (2013).
8. A. J. Lelis et al., *IEEE Trans. Elec. Dev.* **55**(8), 1835 (2008).
9. B. Lu and T. Palacios, *IEEE Elec. Dev. Lett.* **31**(9), 951 (2010).
10. K. Shenai et al., *IEEE Trans. Elec. Dev.* **36**(9), 1811 (1989).
11. W. Shockley, *Solid-State Elec.* **2**(1), 35 (1961).
12. S. Bajaj et al., *Appl. Phys. Lett.* **105**, 263503 (2014).
13. J. L. Hudgens et al., *IEEE Trans. Power Elec.* **18**(3), 907 (2003).
14. E. Bellotti and F. Bertazzi, *J. Appl. Phys.* **111**, 103711 (2012).
15. G. E. Stillman and C. M . Wolfe, in *Semiconductors and Semimetals*, R. K. Willardson and A. C. Beer, Eds., v. 12, p. 291, Academic Press, New York (1977).
16. T. Paskopva et al., *Proc. IEEE* **98**(7), 1324 (2010).
17. T. J. Anderson et al., *Elec. Lett.* **50**(3), 197 (2014).
18. J. Xie et al., *Phys. Stat. Sol. C* **8**(7-8), 2407 (2011).
19. I. C. Kizilyalli et al., *IEEE Trans. Elec. Dev.* **60**(10), 3067 (2013).
20. I. C. Kizilyalli et al., *IEEE Elec. Dev. Lett.* **35**(2), 247 (2014).
21. I. C. Kizilyalli et al., *IEEE Trans. Elec. Dev.* **62**(1), 414 (2015).
22. S. Chowdhury et al., *Semi. Sci. Tech.* **28**, 074014 (2013).
23. H. Ohta et al., *IEEE Elec. Dev. Lett.* **36**(11), 1180 (2015).
24. Z. Hu et al., *Appl. Phys. Lett.* **107**, 243501 (2015).
25. J. R. Dickerson et al., *IEEE Trans. Elec. Dev.* **63**(1), 419 (2016).
26. M. P. King et al., *IEEE Trans. Nuc. Sci.* **62**(6), 2912 (2015).
27. A. A. Allerman et al., *J. Cryst. Growth* **388**, 76 (2014).
28. A. Raman et al., *Jap. J. Appl. Phys.* **47**(5), 3359 (2008).
29. T. Nanjo et al., *Appl. Phys. Lett.* **92**, 263502 (2008).
30. T. Nanjo et al., *IEEE Trans. Elec. Dev.* **60**(3), 1046 (2013).
31. S. Hashimoto et al., *Phys. Stat. Sol. C* **7**(7-8), 1938 (2010).
32. S. Hashimoto et al., *SEI Tech. Rev.* **71**, 83 (2010).
33. H. Tokuda et al., *Appl. Phys. Exp.* **3**, 121003 (2010).
34. S. Hashimoto et al., *Phys. Stat. Sol. A* **209**(3), 501 (2012).
35. N. Yafune et al., *Elec. Lett.* **50**(3), 211 (2014).
36. H. Hahn et al., *Semi. Sci. Tech.* **28**, 074017 (2013).
37. J. P. Ibbetson et al., *Appl. Phys. Lett.* **77**, 250 (2000).